Hindawi
Complexity
Volume 2023, Article ID 9812174, 1 page
https://doi.org/10.1155/2023/9812174

Retraction

Retracted: Meso-Complexity Computer Simulation Investigation on Antiexplosion Performance of Double-Layer Foam Aluminum under Pore Grading

Complexity

Received 19 December 2023; Accepted 19 December 2023; Published 20 December 2023

This article has been retracted by Hindawi following an investigation undertaken by the publisher [1]. This investigation has uncovered evidence of one or more of the following indicators of systematic manipulation of the publication process:

(1) Discrepancies in scope
(2) Discrepancies in the description of the research reported
(3) Discrepancies between the availability of data and the research described
(4) Inappropriate citations
(5) Incoherent, meaningless and/or irrelevant content included in the article
(6) Manipulated or compromised peer review

The presence of these indicators undermines our confidence in the integrity of the article's content and we cannot, therefore, vouch for its reliability. Please note that this notice is intended solely to alert readers that the content of this article is unreliable. We have not investigated whether authors were aware of or involved in the systematic manipulation of the publication process.

Wiley and Hindawi regrets that the usual quality checks did not identify these issues before publication and have since put additional measures in place to safeguard research integrity.

We wish to credit our own Research Integrity and Research Publishing teams and anonymous and named external researchers and research integrity experts for contributing to this investigation.

The corresponding author, as the representative of all authors, has been given the opportunity to register their agreement or disagreement to this retraction. We have kept a record of any response received.

References

[1] Z. Wang, W. B. Gu, X. B. Xie, Y. T. Chen, and L. Fu, "Meso-Complexity Computer Simulation Investigation on Antiexplosion Performance of Double-Layer Foam Aluminum under Pore Grading," *Complexity*, vol. 2020, Article ID 4121926, 13 pages, 2020.

Hindawi
Complexity
Volume 2020, Article ID 4121926, 13 pages
https://doi.org/10.1155/2020/4121926

Research Article

Meso-Complexity Computer Simulation Investigation on Antiexplosion Performance of Double-Layer Foam Aluminum under Pore Grading

Zhen Wang, Wen Bin Gu, Xing Bo Xie, Yu Tian Chen, and Lei Fu

Army Engineering University of PLA, Nanjing 210007, China

Correspondence should be addressed to Wen Bin Gu; 1120122090@bit.edu.cn

Received 12 July 2020; Revised 19 August 2020; Accepted 14 September 2020; Published 22 September 2020

Academic Editor: Zhihan Lv

Foam aluminum is an energy-absorbing material with excellent performance. The interlayer composed of multiple layers of foam aluminum and steel plate has good antiexplosion ability. In order to explore the antiexplosion performance of double-layer foam aluminum under different porosity rankings and to reveal its microscopic deformation law and failure mechanism, three kinds of aluminum foams with a porosity of 80%, 85%, and 90% were selected to form six different structures. Based on the Voronoi algorithm, a three-dimensional foam aluminum generation algorithm with random pore size and random wall thickness was written by using the Python language and Fortran language. The three-dimensional mesoscopic model of double-layer closed-cell aluminum foam sandwich panel is established by using LS-DYNA and ABAQUS software. The explosion process was simulated, and the flow field movement of explosion shock wave of aluminum foam under different porosity rankings was analyzed. Two groups of aluminum foam were randomly selected for the explosion test and compared for the strain and compression. The test results are consistent with the simulation results, which verifies the correctness of the three-dimensional meso-model. The results show that when the porosity of the upper layer of aluminum foam is greater than that of the lower layer of aluminum foam, the sandwich structure of double-layer aluminum foam has a large compression and the bottom plate has a small displacement; it is not that the greater the compression amount of aluminum foam is, the better the antiexplosion and wave absorption ability is. When the aluminum foam reaches the ultimate load-bearing capacity, the aluminum foam transfers the load due to compaction, resulting in stress enhancement phenomena. Through the analysis of the compression amount, floor deformation, wave dissipation capacity, and energy ratio of aluminum foam, it is concluded that the antiexplosion wave absorption effect of the sandwich structure of aluminum foam with 80%/85% group is the best; the changes of porosity and cell wall are important factors affecting the energy absorption capacity of aluminum foam.

1. Introduction

In recent years, various explosions have occurred frequently. Explosion containment vessels (ECVs) are widely used to completely contain the effects of explosions. Foamed aluminum (ALF) is a kind of solid material based on aluminum or aluminum alloy with three-dimensional polyhedral holes randomly distributed inside [1–4]. Because of its special porous properties, aluminum foam can have a very long and almost unchanged platform compression section during compression. While the strain increases gradually, the stress in the compression zone of the platform basically remains unchanged and can absorb a lot of energy, so aluminum foam is an excellent energy-absorbing material [5–7], which has a good effect on reducing stress waves [8]. It has been widely used in all aspects of explosion shock protection [9–12].

The sandwich type structures, comprising the aluminum foams in the core and the thin steel cover plates, have been used to withstand higher impulse under intense dynamic events. By attaching the sandwich structure containing aluminum foam in the middle to the protective engineering or the outer surface of the building, under the impact load, the upper panel directly

acted by the external load produces a shock wave and then compresses the internal aluminum foam material; it leads to the deformation and buckling of aluminum foam, which absorbs energy, protects the bunker target, and resists the impact effect and explosion damage caused by strong dynamic load [8, 13–16]. Many scholars have studied the dynamic response and energy absorption capacity of metal foam sandwich structure, especially under explosive loading [17–21]. The results show that the dynamic properties of metal foams are affected by many factors, such as meso-structure (density, core gradation, cell wall strength, etc.), plate thickness, and loading strain rate. Functionally graded materials optimize their properties by controlling the performance gradient [22], and this method can be extended to metal foams with gradient relative density. Mortensen et al. [23, 24] made sandwich multilayer aluminum foam with core relative density $\rho/\rho_s = 150.45\%$ and found that density classification does provide weight reduction in some strength-limited applications. The study [25] shows that the equal density foam shows the conventional behavior of metal foam. Under the condition of high strain, the foam expands to a nearly flat platform area, and then densification occurs, while the density gradient sample shows an obvious positive slope in the plateau region. As we all know, aluminum foam is a highly complex porous material. Its inherent multiscale characteristics and heterogeneity come from randomly distributed cells [26]. The meso-reaction is of great significance to the mechanical behavior of aluminum foam and the energy absorption capacity under impact loading. Li et al. [27] studied the response of gradient honeycomb sandwich structure under explosive loading by means of experiment and numerical simulation. It was found that, under the same conditions, graded sandwich plate had better antiexplosion ability than ungraded Sandwich plate. When the sandwich plate is arranged in the order of decreasing relative density, the energy absorption capacity of the sandwich plate and the attenuation effect of the contact stress on the back plate are the best. Zhou et al. [28] established a high-speed compression model of aluminum foam based on impact theory and rigid ideal plastic locking model of aluminum foam. Combined with numerical simulation, the energy absorption of gradient aluminum foam under explosive loading was studied. The results show that the larger the density gradient of aluminum foam sandwich is, the smaller the total energy input to aluminum foam is and the smaller the final deformation of aluminum foam is. Dou et al. [29] have studied the strain rate of aluminum foam sandwich panels by means of numerical simulation and think that the strain rate effect of aluminum foam becomes more and more obvious with the increase of relative density. However, the proposed meso-model of aluminum foam also has some shortcomings. Based on the three-dimensional Voronoi algorithm technology, many scholars [30–32] have established a three-dimensional meso-model of aluminum foam, which can well simulate the random distribution of aluminum foam pores and greatly promote the study of three-dimensional meso-mechanical properties of aluminum foam. However, for the meso-model of aluminum foam established by three-dimensional Voronoi algorithm, most of the hole walls are shell elements, and their thickness is the same at any position, which obviously does not accord with the experimental results. In order to simulate the deformation and failure process of aluminum foam more truly under external load, it is very necessary to establish a wall thickness model.

2. Three-Dimensional Mesoscopic Modeling of Double-Layer Aluminum Foam Sandwich Panel

In this chapter, we consider the cells in the foam and give the generation algorithm of the three-dimensional model of double-layer closed-cell aluminum foam. The algorithm consists of three steps. Firstly, the random polyhedron is modeled and the geometric features are extracted; then, a three-dimensional random aluminum foam generation algorithm is developed to control the random wall thickness of the pore wall, and the aluminum foam mesh model is established by reading it into the TrueGrid software. Finally, the three-dimensional mesoscopic model of aluminum foam is imported into the LS-DYNA software to establish the explosion model of double-layer aluminum foam sandwich panel.

2.1. Modeling Method of Three-Dimensional Meso-Model of Aluminum Foam. In this paper, based on the three-dimensional Voronoi algorithm technology, the discrete data points are connected reasonably, the Delaunay triangulation is constructed, and the vertical bisector of the two adjacent points is connected to form the Tyson polygon [33]. The pores of the aluminum foam are regarded as the interior of the Tyson polygon, and the outline of the polygon is regarded as the cell wall of the aluminum foam. Because the wall thickness of aluminum foam is random and uneven, the random polyhedron is modeled by ABAQUS software, and the geometric features of the model are extracted. Then, based on the Voronoi algorithm, a three-dimensional foam aluminum generation algorithm with random pore size and random wall thickness was written using Python language and Fortran language. The geometric boundary parameters were read, and the random wall thickness was set to better simulate the foam aluminum under real conditions. The model uses TrueGrid's excellent grid filling technology to build a meso-grid model of aluminum foam. The finite element model of aluminum foam is obtained, as shown in Figure 1.

2.2. Material Model and Parameters. The bottom plate, sleeve, bracket, and end cover of the system are made of Q235 steel. The above materials and aluminum foam are numerically simulated by PLASTIC KINEMATIC material model. The model can well describe the mechanical

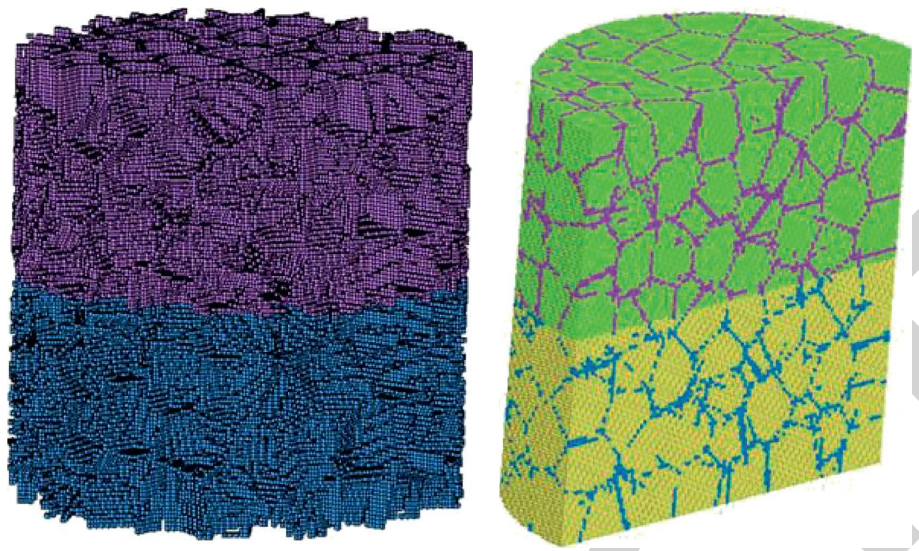

(a) (b)

Figure 1: Three-dimensional microscopic view of double-layer foam aluminum.

Table 1: Metal material parameters.

Metallic material	q (kg/m^3)	E (GPa)	μ	SIGY (MPa)	ETAN (GPa)
Q235 steel	7830	210	0.274	235	6.1
Aluminum foam	2730	70	0.34	185	4.62

properties of metal materials and is widely used in numerical calculation. The calculated parameters of the metal are shown in Table 1.

The air uses the ∗ MAT_NULL material model, and the equation of state is described using ∗ EOS_LINEAR_POLYNOMIAL. The expression of the equation of state is as follows:

$$p = C_0 + C_1\mu + C_2\mu^2 + C_3\mu^3 + \left(C_4 + C_5\mu + C_6\mu^2\right)E,$$
$$\mu = \left(\frac{1}{V}\right) - 1 = \left(\frac{\rho}{\rho_0}\right) - 1, \quad (1)$$
$$C_4 = C_5 = \gamma - 1.$$

Considering air as the gas in an ideal state, the coefficients of the polynomial equation are $C_0 = C_1 = C_2 = C_3 = C_6 = 0$. The variable coefficient γ is often set to 1.4, so $C_4 = C_5 = 0.4$. E_0, ρ_0, and V_0 are the initial energy density, the initial density, and the initial relative volume parameter values which are 1.29 g·cm^{-3}, 0.25 MPa, and 1.0. The parameters are shown in Table 2.

The high-energy combustion explosives use ∗ MAT_HIGH_EXPLOSIVE_BURN material model, and the equation of state uses ∗ EOS_JWL to represent the pressure of the explosive product. The expression of the equation of state is shown in the following formula [18]:

Table 2: Material model and EOS parameters of air [20, 34, 35].

C_0 (MPa)	C_1	C_2	C_3	C_4	C_5	C_6	ρ (kg/m^3)
−0.1	0	0	0	0.4	0.4	0	1.225

$$p = A\left(1 - \left(\frac{\omega}{R_1V}\right)\right)e^{-R_1V} + B\left(1 - \left(\frac{\omega}{R_2V}\right)\right)e^{-R_2V} + \left(\frac{\omega E}{V}\right), \quad (2)$$

where E and V are energy density and relative volume, respectively. When the initial calculation is performed, they should be given initial values E_0 and V_0; A, B, and E_0 are pressure units; R_1, R_2, OMEG, and V_0 are dimensionless. The specific material parameters are shown in Table 3.

The outer boundary of the air adopts a nonreflective boundary, the bottom of the bottom plate is set as a fixed boundary, and the contact setting is set: the cover plate is bound to connect with the bottom plate, ∗ CONTACT_TIED_SURFACE_TO_SURFACE, cover plate is connected with aluminum foam, and the aluminum foam is automatically contacted with the bottom plate by automatic surface contact ∗ CONTACT_AUTOMATIC_SURFACE_TO_SURFACE.

2.3. Modeling of Double-Layer Aluminum Foam Sandwich Panel. The energy absorption effect and explosion resistance of aluminum foam are closely related to the density, and the

Table 3: Material model parameters and JWL parameters of TNT.

ρ (kg/m^3)	A (GPa)	B (GPa)	R_1	R_2	PCJ (GPa)	E (J/m^3)	D (m/s)	υ	Ω
1500	347.6	3.39	4.15	0.95	17.92	6.34e9	6957.2	1.0	0.28

difference of porosity will inevitably lead to the change of the density of aluminum foam. The arrangement of different porosity of multilayer aluminum foam will also have a significant impact on the dynamic response of aluminum foam sandwich panels. Six groups of different structures were obtained by permutation and combination of aluminum foam with three densities, namely, 80%, 80%, 85%, 85%, 85%, 90%, 90%, 90%, 90%, 80%, and 90%, respectively. The numerical model is shown in Figure 2. In the model, the mass of the charge is fixed as 520 g, the density is 1.601 g, the radius is 0.086 m, and the spherical charge and the height of the charge are fixed as 25 cm. The thickness of cover plate is fixed at 10 mm, the total height of aluminum foam sandwich is fixed at 78 mm, and the height of single layer is 39 mm. As shown in Figure 2, the bottom plate support of the model is set as a fixed constraint, and a downward prestressed load is applied on the upper surface to clamp the aluminum foam. The pore sizes $R_{\min}$ and $R_{\max}$ in the model are 1 mm and 3 mm, respectively, and the average pore size is 2 mm. In order to ensure the calculation accuracy of the flow field in the container, the element size in the finite element model is 0.2 mm.

2.4. Layout of Measuring Points. After the explosion of the explosive, the explosion products and shock waves of high temperature and high pressure will be produced, which will have a strong destructive effect on the surrounding structures. A measuring point is set up in the sandwich structure bearing the explosion shock wave to test the strength of the stress wave. The location of the measuring points is shown in Figure 3, and three groups of stress measuring points are set. The stress wave intensities of the cover plate were transmitted to the first layer of aluminum foam, the first layer of aluminum foam to the second layer of aluminum foam and the second layer of aluminum foam to the bottom plate are measured, respectively, and the test results are recorded as σ_1, σ_2, and σ_3, respectively. σ_1 is the mean stress of the uppermost element of the first layer of aluminum foam, σ_2 is the average stress of the lowest element of the first layer and the uppermost element stress of the second layer, and σ_3 is the mean stress of the uppermost element of the bottom plate.

3. Validation

3.1. Experiment Setup. In this paper, the explosion test device shown in Figure 4 is designed to study the anti-explosion performance of double-layer aluminum foam sandwich structure. The shock wave produced by the explosion of the spherical TNT charge causes the cover plate to move and deform and compress the aluminum foam under the explosion load. In the experiment, the blasting height of the charge is fixed at 25 cm, the thickness of the upper panel is fixed at 10 mm, the height of each layer of aluminum foam is 39 mm, and the total thickness of the aluminum foam sandwich is fixed as 78 mm.

In order to evaluate the explosion resistance of different aluminum foam sandwich structures, a cylindrical pressure sensor is installed on the upper surface of the base plate. According to the fixed mode of the whole device, strain gauges are set at the positions of S1, S2, and S3 on the lower surface of the base plate, which mainly test the dynamic response of the bottom plate under the explosion impact load. As shown in Figure 5, the load and deformation of the bottom plate are monitored, respectively. The pressure sensor is in the center of the upper surface of the base plate. The strain gauge S1 is in the center of the lower surface of the base plate.

3.2. Comparative Analysis with the Test. In order to verify the correctness of the model, the strain test values of 80%/90% group and 80%/85% group of aluminum foam were randomly selected and compared. Figure 6 is the comparison diagram of the strain time history curve of 80%/90% foam aluminum test value and simulation value of each measuring point. S1 (2, 3)-e represents the experimental value, and S1 (2, 3) represents the simulation value. As can be seen from the chart, the strain peak value of each measuring point has little difference, and the trend of the strain curve waveform is the same, which tends to be smooth with the increase of time. The test simulation results verify the test results. Figure 7 shows the test height and simulation height of 80% ram 85% aluminum foam after compression. The initial height of double-layer aluminum foam is 78 mm. After the test, the height of double-layer aluminum foam becomes 46.55 mm, and the compression amount is 31.45 mm. The compression amount of the numerical simulation is 32.8 mm, and the difference between the experimental value and the simulation value is small, which can verify the correctness of the model.

4. Analysis of Energy Absorption Mechanism of Aluminum Foam

4.1. Analysis of the Movement Process of Double-Layer Foam Aluminum. This section explores the motion process of 85%/90% foam aluminum sandwich panels under explosive loading.

In the first stage, the explosive center detonates until the shock wave reaches the cover plate and begins to compress the aluminum foam. As shown in the figure, during 0 ms, the explosive initiates at a single point center, and the shock wave front begins to expand outward with the sphere as the center, reaching the cover plate at a certain time between 0.07 ms and 0.08 ms, and the cover plate obtains a certain speed to compress the aluminum foam downward, as shown

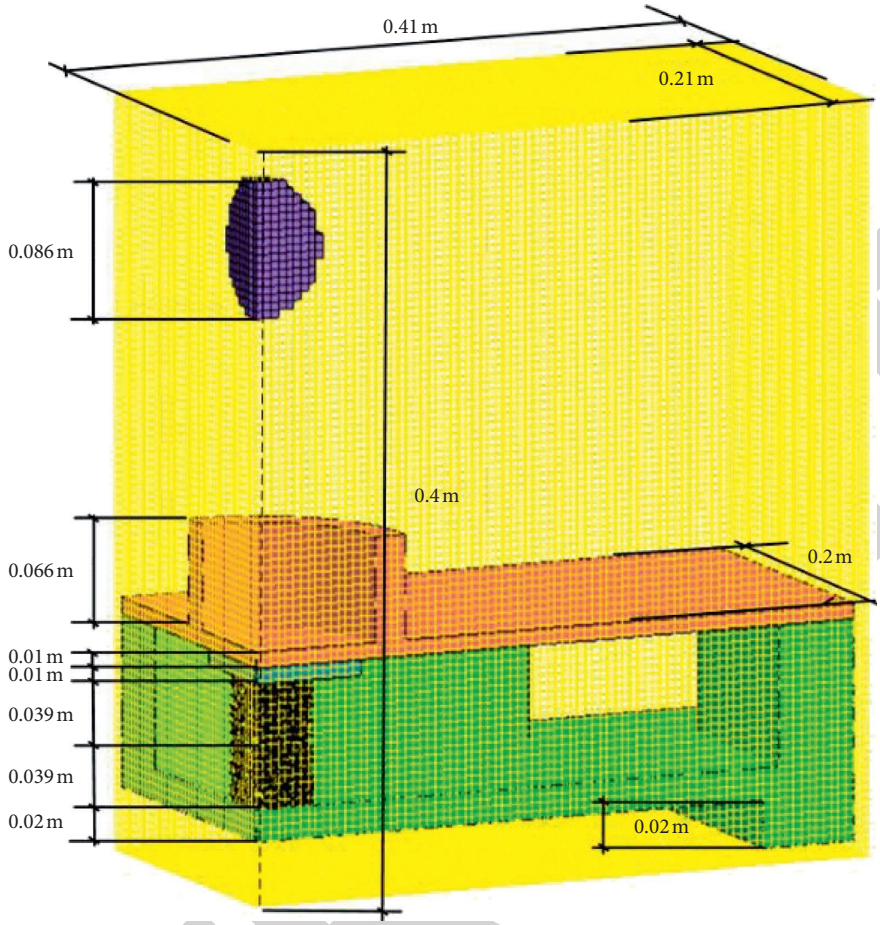

Figure 2: Double-layer aluminum foam sandwich (AFS) structure.

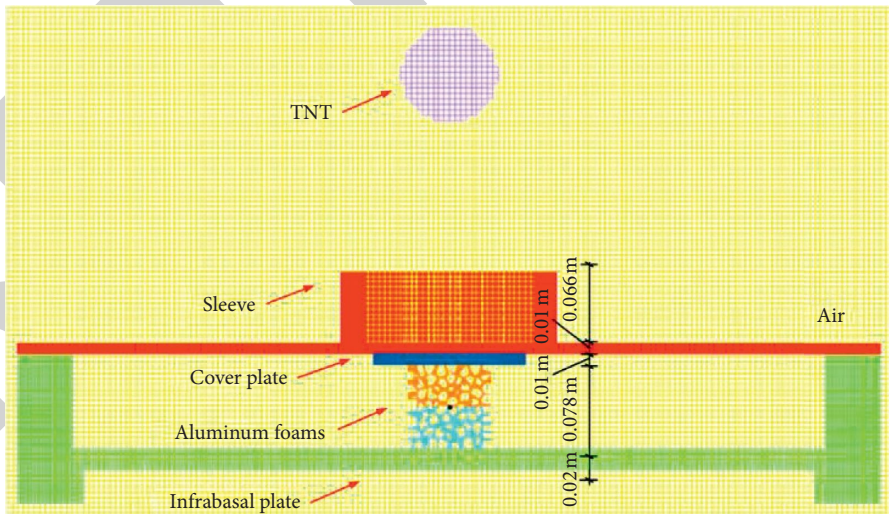

Figure 3: Stress measuring point arrangement.

in the pressure cloud diagram of aluminum foam on the right side of Figure 8.

In the second stage, the cover plate begins to compress aluminum foam to fully compress double-layer aluminum foam. As shown in Figure 9, contact compression occurs at the delamination interface at 0.08 ms, and the stress wave begins to travel from the top foam to the bottom foam, resulting in reflected and transmitted waves. Because the wave impedance of 90% porosity aluminum foam is less than 80% porosity aluminum foam, and 90% porosity is high, so 90% porosity aluminum foam absorbs most of the energy and produces great deformation. The stress wave is

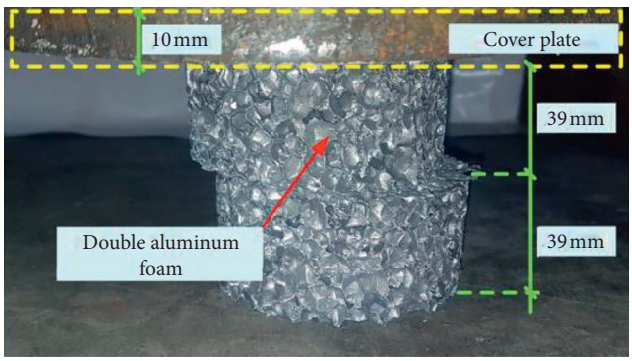

Figure 4: Sandwich plate antiexplosion test device.

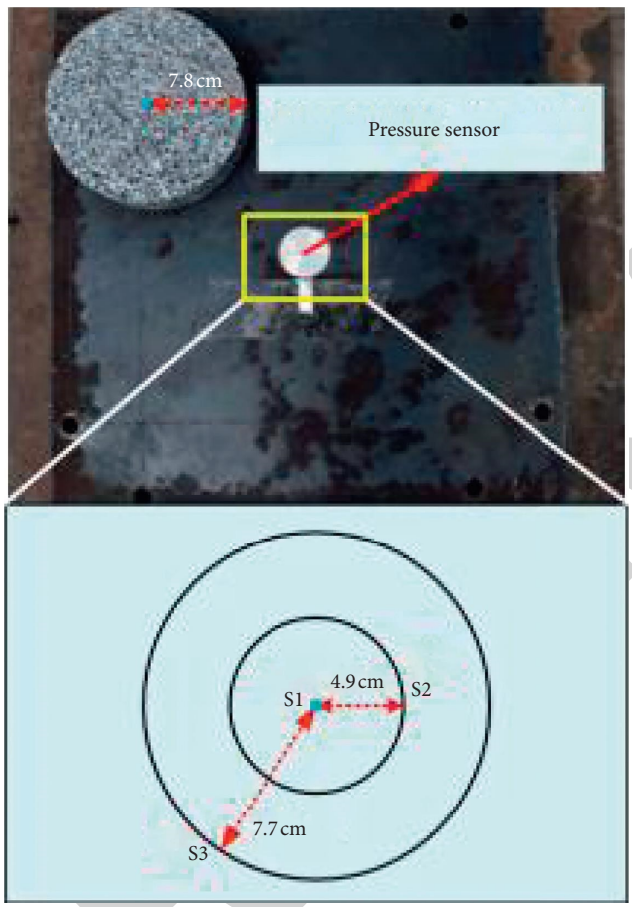

Figure 5: Sensor settings.

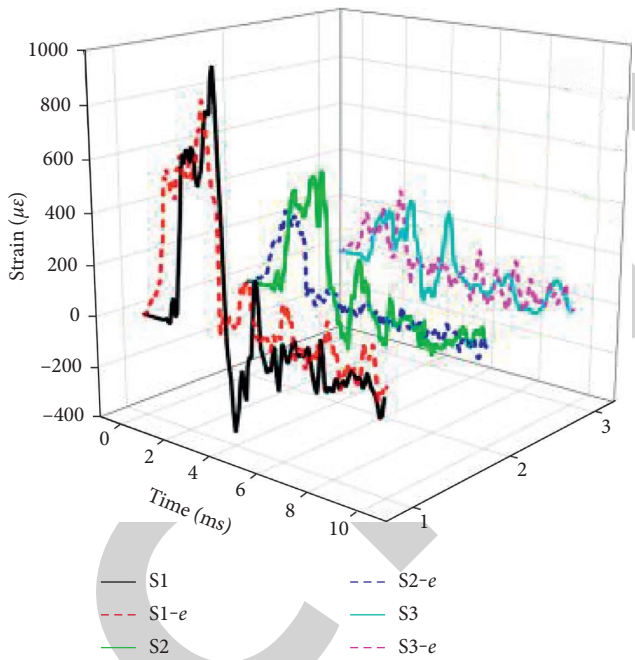

Figure 6: 80%/90% foam aluminum strain diagram.

Figure 7: 80%/85% aluminum foam compression.

transmitted to the bottom plate at 0.24 ms and begins to act to the bottom plate, so that the floor begins to compress and deform. During the explosion process to 1.0 ms, we can see that 90% aluminum foam is completely compressed almost at some time between 1.0 ms and 1.24 ms, while, after 1.0 ms, 80% aluminum foam is compressed as the main energy-absorbing material. This is very helpful for us to study the energy absorption mechanism of layered aluminum foam.

From the summary of the previous research background, we can see that the stress-strain performance of aluminum foam is different under the sorting condition of different aluminum foam density, but the simulation analysis of the ordering of density gradient is still less. In order to further analyze the effect of density gradient on the mechanical properties of closed-cell aluminum foam, this section is based on a three-dimensional meso-model to study the explosion resistance of aluminum foam specimens under different density order and the energy absorption characteristics of aluminum foam with different density gradient under explosive impact loading.

4.2. Analysis of Delamination Characteristics of Double-Layer Aluminum Foam. You can see significant compression when the time reaches 0.48 ms. When compressed to 1.24 ms, the compression of aluminum foam is completed. Figure 10 shows the deformation distribution of aluminum foam under explosive loading under six groups of porosity combinations during 1.24 ms. It can be seen from the figure that the deformation of aluminum foam in 90%/80% group is the largest, with a deformation amount of 34.23 mm. The deformation of the pore wall of aluminum foam is mainly concentrated in the area with large porosity. Through the

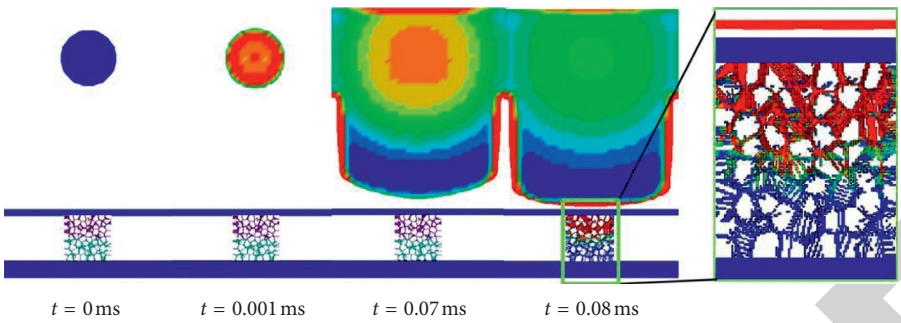

Figure 8: Compressed foam aluminum cover.

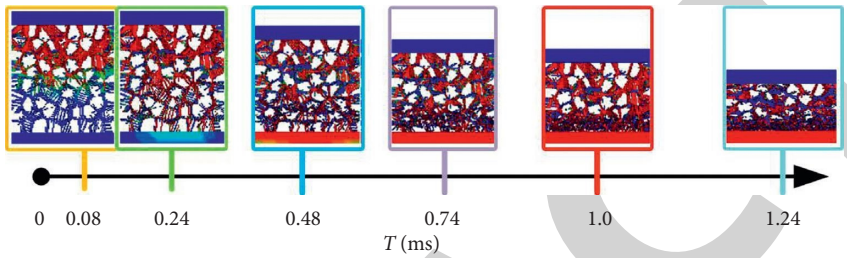

Figure 9: Compressed foam aluminum cover.

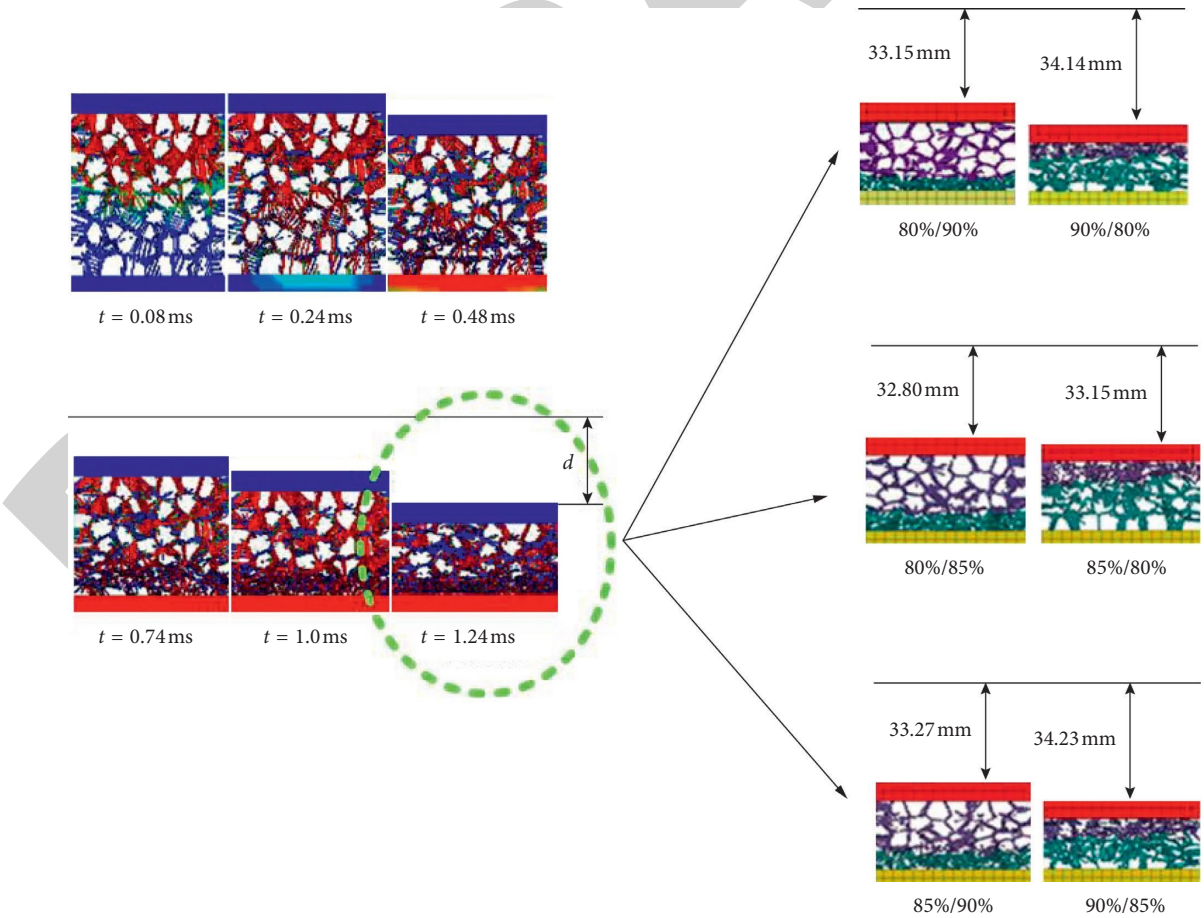

Figure 10: Deformation analysis of six groups of structures.

comparison of the structures of each group, it is found that if the porosity of the upper layer aluminum foam is higher than the lower layer aluminum foam, the compression amount of the double-layer aluminum foam sandwich structure is larger, such as group 90%/80% and group 90%/85%. When the porosity of the upper layer aluminum foam is small, the two layers of aluminum foam begin to deform at the same time, but when the porosity of the upper layer aluminum foam is larger, it will not begin to deform at the same time. Before the upper layer of aluminum foam is compressed to a certain extent, the contact stress between the two layers of aluminum foam is greater than the yield stress of the lower layer of aluminum foam, and the lower layer of aluminum foam begins to deform.

As can be seen from Table 4, the maximum peak displacement of the 90%/80% group is the largest among the six groups, followed by the 90%/85% group displacement. The order of the bottom plate displacement under each combination is as follows: 80%/90% < 85%/90% < 80%/80% < 90%/85% < 90%/85% < 90%/80%. Under the only combination of the two groups of porosity, the large upper porosity will increase the compression of the sandwich structure of double-layer aluminum foam and reduce the displacement of the bottom plate. With the increase of time, the elastic deformation of the bottom plate ends and enters the plastic deformation stage, and the deformation of the bottom plate tends to be stable. After reaching stability, the minimum displacement of the bottom plate is 80%/90% group, followed by 85%/90% group. The order of displacement is as follows: 80%/85% < 85%/90% < 80%/80% < 90%/80% < 90%/85% < 90%/80%. Since the bottom plate displacement of the aluminum foam in the 80%/85% group is the smallest after the stress balance, it is considered that the reorganization is the total optimal group of the six groups. It can be found that, under the positive sequence of porosity, the displacement of the bottom plate is smaller. By comparing the compression amount of aluminum foam, it can be found that the compression amount of aluminum foam in the group of 90%/85% is the largest, but the deformation of the bottom plate is not the smallest, but very large. This also shows that it is not that the greater the compression amount of aluminum foam is, the better the antiexplosion and wave-absorbing ability is and the better the protective effect on the substructure is. The analysis shows that after the aluminum foam reaches the ultimate bearing capacity, the aluminum foam produces stress enhancement due to compaction, so the compression amount of aluminum foam is the largest, but its wave absorption capacity is not the best.

In order to quantitatively describe compressive quantities of double-layer aluminum foams and compare compressive quantities of single-layer aluminum foams, we draw a curve of displacement time history of different porosity combinations in Figure 11. It can be seen from graphs that foam aluminum reaches maximum displacement rapidly during elastic stage and then decreases and eventually tends to be smooth. Results show that compressive strength of double-layer foamed aluminum bottom plate is smaller than that of single-layer aluminum foam plate. Design of double-layer aluminum foam can improve antiexplosion property of

Table 4: Displacement of double-layer foamed aluminum under each combination.

	80/90	90/80	80/85	85/80	90/85	85/90
Maximum deformation	−1.57	−2.01	−1.76	−1.84	−1.94	−1.61
Deformation after equilibrium	−1.00	−1.55	−0.28	−1.17	−1.51	−0.54

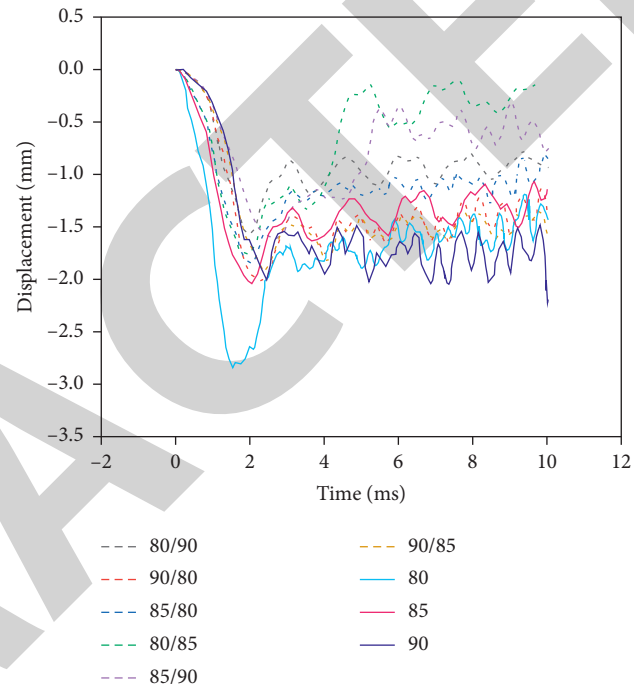

Figure 11: Displacement of single-layer aluminum foam bottom plate.

Table 5: Upper aluminum foam energy.

	80/90	80/85	90/80	90/85	85/80	85/90
Total energy (J)	688.11	739.35	584.55	503.74	970.24	898.67
Internal energy (J)	604.19	665.91	556.76	467.01	952.9	846.21
Kinetic energy (J)	83.92	73.44	27.79	36.73	17.34	52.46

Table 6: Energy of aluminum foam in the lower layer.

	80/90	80/85	90/80	90/85	85/80	85/90
Total energy (J)	1125.98	1734.18	1322.07	1125.98	1154.61	1605.32
Internal energy (J)	1064.42	1096.89	1240.25	1031.1	1085.62	1477.88
Kinetic energy (J)	61.56	637.29	81.82	94.88	68.99	127.44

Table 7: Floor energy.

	80/90	80/85	90/80	90/85	85/80	85/90
Total energy (J)	126.12	121.55	249.56	191.24	162.37	176.41
Internal energy (J)	83.14	102.59	187.11	141.62	125.78	133.26
Kinetic energy (J)	42.98	18.96	62.45	49.62	36.59	43.15

aluminum foam effectively, eliminate partial explosion shock wave effectively, and play positive role in protecting lower structure.

4.3. Energy Analysis. Tables 5–7 provide energy for upper and lower aluminum foams and bottom plates, respectively. According to the tables, the total energy of lower aluminum foam is higher than that of upper aluminum foam, which is consistent with wave dissipation rule of aluminum foam at upper and lower level. The fluctuation dissipation rate of low aluminum foam is obviously higher than that of aluminum foam. As shown in Table 5, the difference between total energy and internal energy is smaller than that of upper foam aluminum, and the kinetic energy of 80%/90% group is maximum, which is consistent with minimum law of peak displacement of bottom plate of upper foam aluminum group, followed by group 80%/85%. As shown in Table 6, the gap between total energy and internal energy is larger during lower aluminum foams. The maximum kinetic energy is in group 80%/85%, and the minimum kinetic energy is in group 80%/90%. As shown in Table 7, total energy, internal energy, and kinetic energy are minimal in group 80%/85%. The results show that porosity has great influence on energy absorption characteristics of samples; when the total energy of aluminum foam increases, the energy of bottom plate decreases. There are mainly two types of aluminum foam to improve porosity; one case is pore quantity that increases; another case is pore wall thickness that decreases. Therefore, more cell walls produce larger deformation plastic strain absorbing more energy under the same strain condition. However, due to low porosity, the overall antiblast performance of this device is better but critical point of complete compression and incomplete compression can be found which ensures that load can be absorbed completely without destroying floor.

Figure 12 shows the ratio of internal energy to kinetic energy of the floor arranged at all levels of density. It can be seen from the diagram that the energy ratio of the floor fluctuates with the increase of time, indicating that the kinetic energy ratio of the floor continues to decrease and the kinetic energy is converted into internal energy and finally tends to be stable. The soleplate of 80%/85% group showed the maximum peak of energy ratio during 4.496 ms, and obvious secondary damage occurred at the interface, resulting in secondary work done by aluminum foam, so it consumes a lot of energy. Since the displacement of the bottom plate of the 80%/85% group is the smallest, it can be concluded that this group is the best group in density order.

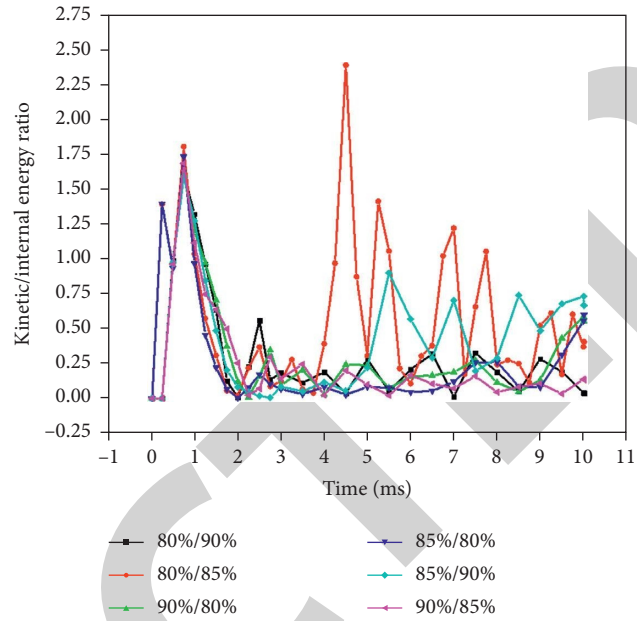

Figure 12: Energy ratio of aluminum foam.

5. Investigation on Three-Dimensional Meso-Mechanical Properties of Double-Layer Aluminum Foam Sandwich Panels

In order to analyze the relationship between meso-parameters and mechanical properties of materials under explosive loading, we study the energy absorption characteristics of aluminum foam materials and the effects of meso-failure mechanism of aluminum foam cell wall on its antiexplosion performance and energy absorption. In this section, the dynamic mechanical properties of aluminum foam specimens are studied by simulating the double-layer aluminum foam sandwich panel under explosive load.

The literature research [36] shows that the stress wave propagates from one medium to another; if the wave impedance of the two media is different, then the stress wave will be reflected and transmitted at the interface of the two media, and its intensity satisfies the following relationship:

$$\left(\frac{\sigma_R}{\sigma_I}\right) = \frac{(\rho_2 C_2 - \rho_1 C_1)}{(\rho_2 C_2 + \rho_1 C_1)}, \tag{3}$$

$$\left(\frac{\sigma_T}{\sigma_I}\right) = \frac{(2\rho_2 C_2)}{(\rho_2 C_2 + \rho_1 C_1)}. \tag{4}$$

Among them, σ_I, σ_R, and σ_T represent the incident wave, reflected wave, and transmitted wave intensity of the shock wave at the interface, respectively; $\rho_1 C_1$ represents the wave impedance of the first layer medium, and $\rho_2 C_2$ represents the wave impedance of the second layer medium. It can be seen from formulas (3) and (4) that when the aluminum foam sandwich is delaminated in density, due to the difference of medium wave impedance on both sides of the interface, the shock wave that continues to propagate along the foam

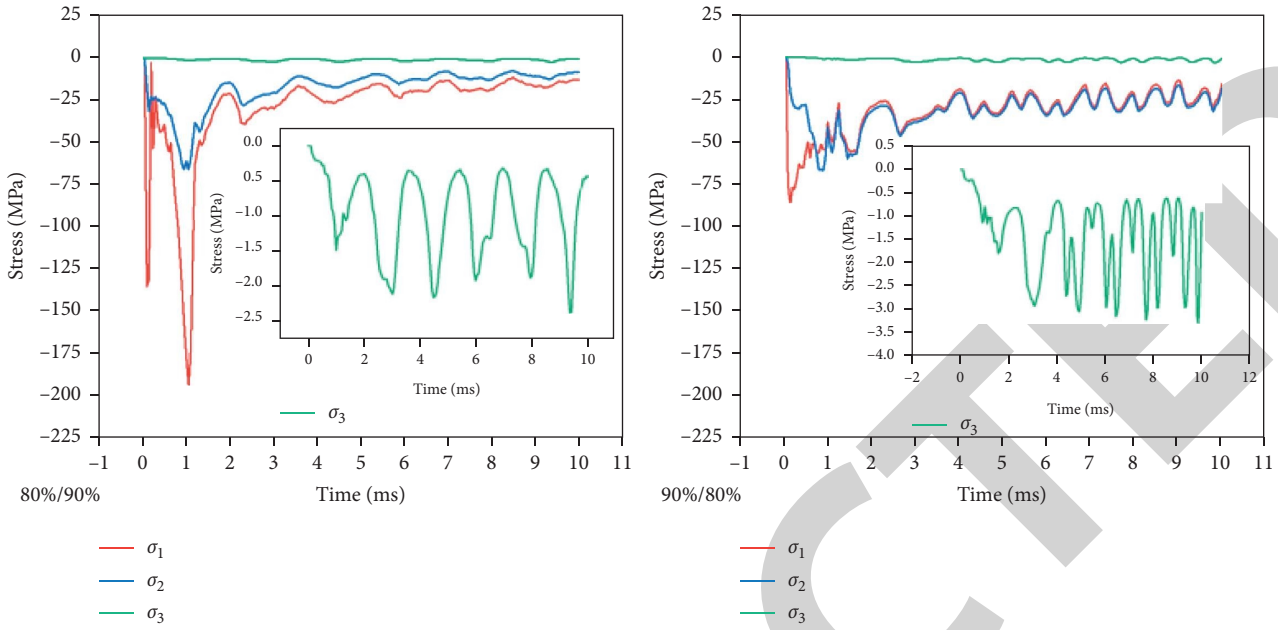

Figure 13: Double-layer aluminum foam with porosity of 80% and 90%.

aluminum to the bottom plate after transmission through the interface decreases, while the shock wave reflected from the interface near the explosion source end may further compress the deformed area of the aluminum foam, so delamination of the aluminum foam may increase the energy absorption value of the sandwich structure core of the foam aluminum sandwich. At the same time, the load acting on the protected structure is reduced. Therefore, we established a three-dimensional mesoscopic model of double-layer aluminum foam and quantitatively analyzed the attenuation effect of stress wave strength of double-layer aluminum foam sandwich structure.

When the porosity combination of aluminum foam is 80% and 90%, the distribution of stress waves in the sandwich structure is shown in Figure 13. Intuitively, in Figure 13, the stress value of the first layer reached 135.94 MPa at 0.102 ms and reached the second peak at 1.057 ms due to emission, indicating that, in the steel plate, the change rate of stress wave is extremely high, the stress wave intensity of the second layer is 31.17 MPa, and the stress wave intensity of the third layer is 2.38 MPa. The attenuation of the explosion shock wave is as high as 77.07% after passing through the first layer of aluminum foam, the attenuation of the explosion wave after passing through the second layer of aluminum foam reaches 92.36%, and the overall wave dissipation rate is 98.25%. The rising edge of the stress wave in the first layer is 10.2 μs, the rising edge of the stress wave in the second layer is 14.9 μs, and the rising edge of the stress wave in the third layer can reach 0.9 ms. After aluminum foam, the rising time of stress wave has been greatly improved. When the porosity of the upper layer of aluminum foam is 90% and the porosity of the lower layer of aluminum foam is 80%, the stress value of the first layer is 86.70 MPa, the attenuation of explosion shock wave after the first layer of aluminum foam is 64.46%, the stress value of explosion wave after the second layer of aluminum foam is 2.94 MPa, the attenuation rate is 90.45%, and the overall wave dissipation rate is 96.61%. It can be found that whether it is the first layer of aluminum foam or the second layer of aluminum foam, the positive sequence arrangement of porosity has higher wave dissipation rate and the phenomenon of interface delamination is more obvious.

When the porosity combination of aluminum foam is 80% and 85%, the distribution of stress waves in the sandwich structure is shown in Figure 14. When the upper porosity of the aluminum foam is 80% and the porosity of the lower aluminum foam is 85%, the stress value of the first layer of the explosion shock wave reaches 158.76 MPa, and the attenuation is as high as 59.07% after passing through the first layer of aluminum foam; the stress value of the explosion wave after passing through the second layer of aluminum foam is 2.38 MPa, the attenuation rate is 95.80%, and the overall wave dissipation rate is 98.51%. When the porosity of the upper layer of aluminum foam is 85% and that of the lower layer is 80%, the stress value of the first layer is 151.01 MPa, and the attenuation rate of the explosion shock wave after the first layer of aluminum foam is 49.02%. After the second layer of aluminum foam, the stress value of the explosion wave is 2.27 MPa, the attenuation rate is 95.34%, and the overall wave dissipation rate is 98.49%. It is also found that whether it is the first layer of aluminum foam or the second layer of aluminum foam, the positive sequence arrangement of porosity has a higher wave dissipation rate and the phenomenon of interface delamination is more obvious.

When the porosity combination of aluminum foam is 85% and 90%, the distribution of stress waves in the sandwich structure is shown in Figure 15. When the porosity of the upper layer of aluminum foam is 85% and that of the lower layer is 90%, the stress value of the first layer is

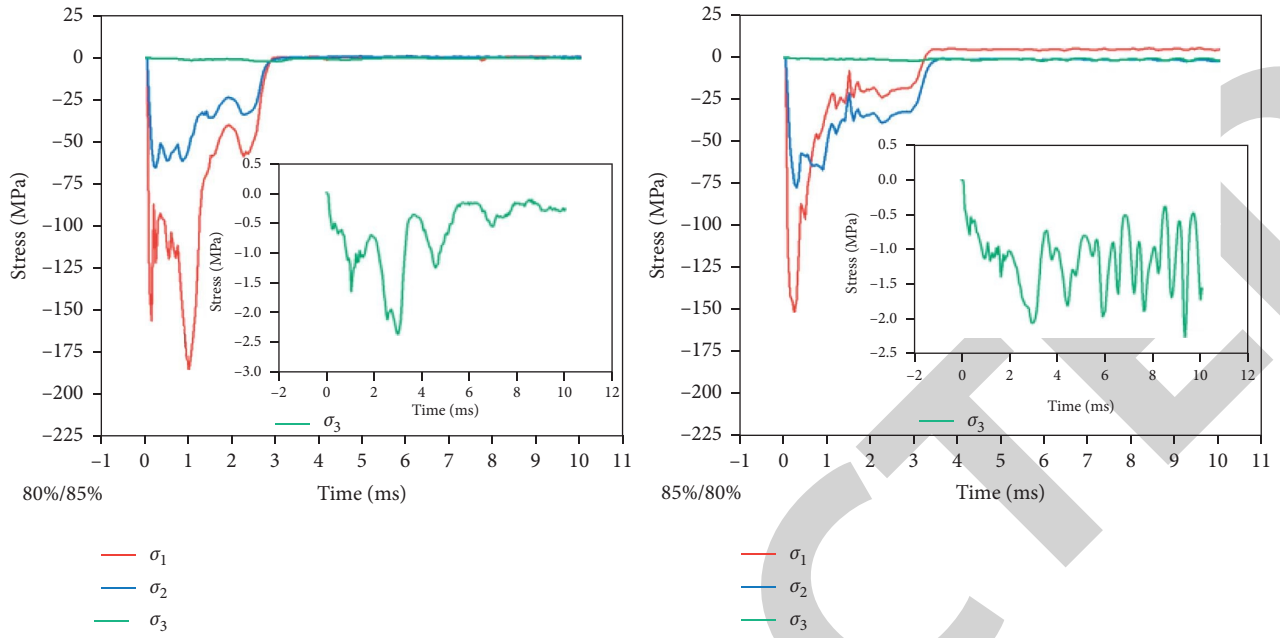

Figure 14: Double-layer aluminum foam with porosity of 80% and 85%.

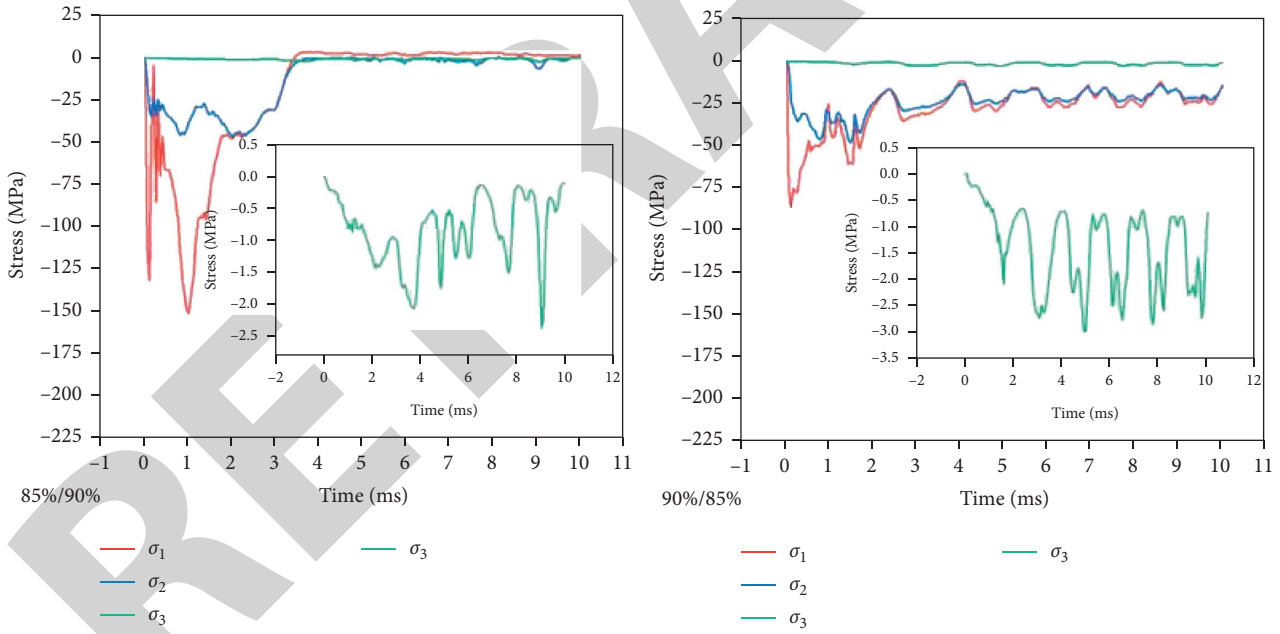

Figure 15: Double-layer aluminum foam with porosity of 85% and 90%.

129.36 MPa. The shock wave of the explosion after the first layer of aluminum foam attenuates by 71.44%. After the second layer of aluminum foam, the stress value of the explosion wave is 2.013 MPa, the attenuation rate is 96.81%, and the overall wave dissipation rate is 98.43%. When the porosity of the upper layer of aluminum foam is 90% and the porosity of the lower layer of aluminum foam is 85%, the stress value of the first layer is 86.63 MPa; the explosion shock wave attenuates 59.15% after the first layer of aluminum foam, and the stress value of the explosion wave after the second layer of aluminum foam is 2.72 MPa; the attenuation rate is 92.31%, respectively, and the overall wave dissipation rate is 96.86%. It is also found that whether it is the first layer of aluminum foam or the second layer of aluminum foam, the positive sequence arrangement of porosity has a higher wave dissipation rate and the phenomenon of interface delamination is more obvious.

Due to different porosity of aluminum foam, different reflection and refraction phenomena occur after explosion wave propagation, so there is stress difference between upper

surfaces of aluminum foam layer. It can be concluded from the above picture that the overall wave dissipation rates of six groups of aluminum foams with different porosity have little difference. By comparison, it is found that the porosity is arranged in positive order, and the difference between the upper and lower layers is small, and the wave dissipation rate of the lower layer aluminum foam is higher. To sum up, the antiexplosion and wave-absorbing ability of the double-layer foam sandwich structure of 80%/85% group is the best, and the greater the porosity is, the better the antiexplosion ability is.

6. Conclusions

In this paper, a three-dimensional mesoscopic model of double-layer aluminum foam sandwich panel is established, and the fluid-solid coupling method is used to analyze the flow field motion of explosion shock wave of aluminum foam with different porosity. A series of conclusions are obtained through numerical simulation and analysis:

(1) On the basis of Voronoi algorithm, the aluminum foam generation algorithm with random three-dimensional pore size and wall thickness is compiled by using Python language and Fortran language. The three-dimensional mesoscopic model of double-layer closed-cell aluminum foam sandwich panel is established by using LS-DYNA and ABAQUS software, and the random wall thickness is set to better simulate the real aluminum foam model.

(2) The strain test values of 80%/90% group and 80%/85% group of aluminum foam were randomly selected and compared with the simulation results. The experimental results are consistent with the simulation results, which verifies the correctness of the three-dimensional meso-model.

(3) Six kinds of three-dimensional mesoscopic models of explosive loading of double-layer aluminum foam with different porosity arrangement were established in LS-DYNA. The numerical simulation results show that, in the group with the same porosity combination, when the porosity of the upper layer aluminum foam is greater than that of the lower layer aluminum foam, the compression amount of the sandwich structure of double-layer aluminum foam is larger, but the displacement of the bottom plate is small; it is not that the greater the compression amount of aluminum foam, the better the antiexplosion and wave absorption capacity. When the aluminum foam reaches the ultimate bearing capacity, the foam aluminum produces stress enhancement due to compaction.

(4) Through the mesoscopic simulation of aluminum foam, it is found that the changes of porosity are very important factors affecting the energy absorption capacity of aluminum foam.

(5) Through the analysis of the compression amount, floor deformation, wave dissipation capacity, and energy ratio of aluminum foam, it is concluded that the antiexplosion wave absorption effect of the sandwich structure of aluminum foam with 80%/85% group is the best.

Data Availability

The drawings and tables in the article are all original data, which are all obtained by experiments and computer simulations. In the future, when readers need the data in the article for secondary development, they can e-mail the authors to provide it. The drawings and tables in the article can be edited without any problems.

Conflicts of Interest

The authors declare that they have no conflicts of interest regarding their work.

Acknowledgments

The financial support from the Science and Technology Innovation Project (KYGYZB0019003) and the Department of Infrastructure Barracks (China) is gratefully acknowledged.

References

[1] I. Duarte, M. Vesenjak, and L. Krstulović-Opara, "Compressive behaviour of unconstrained and constrained integral-skin closed-cell aluminium foam," *Composite Structures*, vol. 154, pp. 231–238, 2016.

[2] J. H. Kim, D. Kim, M.-G. Lee, J. K. Lee, and M.-G. Lee, "Multiscale analysis of open-cell aluminum foam for impact energy absorption," *Journal of Materials Engineering and Performance*, vol. 25, no. 9, pp. 3977–3984, 2016.

[3] B. Hamidi Ghaleh Jigh, H. Hosseini Toudeshky, and M. A. Farsi, "Experimental and multi-scale analyses of open-celled aluminum foam with hole under compressive quasi-static loading," *Journal of Alloys and Compounds*, vol. 695, pp. 133–141, 2017.

[4] M. Vesenjak, C. Veyhl, and T. Fiedler, "Analysis of anisotropy and strain rate sensitivity of open-cell metal foam," *Materials Science and Engineering: A*, vol. 541, pp. 105–109, 2012.

[5] G. Lu and T. X. Yu, *Energy Absorption of Structures and Materials*, Woodhead Publishing Ltd., Cambridge, MA, USA, 2003.

[6] S. Cheng, X. Zhao, B. Xiao, and Y. Xin, "Compression tests on aluminum honeycomb and epoxy resin Sandwich panels," *Emerging Materials Research*, vol. 4, no. 2, pp. 157–164, 2015.

[7] D. K. Rajak, L. A. Kumaraswamidhas, S. Das, and S. Senthil Kumaran, "Characterization and analysis of compression load behaviour of aluminium alloy foam under the diverse strain rate," *Journal of Alloys and Compounds*, vol. 656, pp. 218–225, 2016.

[8] R. P. Merrett, G. S. Langdon, and M. D. Theobald, "The blast and impact loading of aluminium foam," *Materials & Design*, vol. 44, pp. 311–319, 2013.

[9] J. Park and H.-J. Choi, "Experiments and numerical analyses of HB400 and aluminum foam sandwich structure under landmine explosion," *Composite Structures*, vol. 134, pp. 726–739, 2015.

[10] M. F. Ashby, A. G. Evans, N. A. Fleck, L. J. Gibson, and J. W. Hutchinson, *Metal Foams: A Design Guide*, Butterworth-Heinemann, Oxford, UK, 2000.

[11] A. G. Evans, J. W. Hutchinson, and M. F. Ashby, "Multifunctionality of cellular metal systems," *Progress in Materials Science*, vol. 43, no. 3, pp. 171–221, 1998.

[12] M. V. Hosur, U. K. Vaidya, C. Ulven, and S. Jeelani, "Performance of stitched/unstitched woven carbon/epoxy composites under high velocity impact loading," *Composite Structures*, vol. 64, no. 3-4, pp. 455–466, 2004.

[13] G. S. Langdon, D. Karagiozova, M. D. Theobald et al., "Fracture of aluminium foam core sacrificial cladding subjected to air blast loading," *International Journal of Impact Engineering*, vol. 37, pp. 638–651, 2018.

[14] G. W. Ma and Z. Q. Ye, "Energy absorption of double-layer foam cladding for blast alleviation," *International Journal of Impact Engineering*, vol. 34, no. 2, pp. 329–347, 2007.

[15] G. S. Langdon, D. Karagiozova, M. D. Theobald et al., "Fracture of aluminium foam core sacrificial cladding subjected to air-blast loading," *International Journal of Impact Engineering*, vol. 37, no. 6, pp. 638–651, 2010.

[16] J. A. Main and G. A. Gazonas, "Uniaxial crushing of sandwich plates under air blast: influence of mass distribution," *International Journal of Solids and Structures*, vol. 45, no. 7-8, pp. 2297–2321, 2008.

[17] M. Peroni, G. Solomos, and V. Pizzinato, "Impact behaviour testing of aluminium foam," *International Journal of Impact Engineering*, vol. 53, pp. 74–83, 2013.

[18] L. Jing, Z. Wang, and L. Zhao, "Dynamic response of cylindrical sandwich shells with metallic foam cores under blast loading-numerical simulations," *Composite Structures*, vol. 99, pp. 213–223, 2013.

[19] L. Peroni, M. Avalle, and M. Peroni, "The mechanical behaviour of aluminium foam structures in different loading conditions," *International Journal of Impact Engineering*, vol. 35, no. 7, pp. 644–658, 2008.

[20] W. Nian, K. V. L. Subramaniam, and Y. Andreopoulos, "Dynamic compaction of foam under blast loading considering fluid-structure interaction effects," *International Journal of Impact Engineering*, vol. 50, pp. 29–39, 2012.

[21] X. Liu, X. Tian, T. J. Lu, D. Zhou, and B. Liang, "Blast resistance of sandwich-walled hollow cylinders with graded metallic foam cores," *Composite Structures*, vol. 94, no. 8, pp. 2485–2493, 2012.

[22] A. Mortensen and S. Suresh, "Functionally graded metals and metal-ceramic composites: part 1 processing," *International Materials Reviews*, vol. 40, no. 6, p. 239, 1995.

[23] A. Pollien, Y. Conde, L. Pambaguian, and A. Mortensen, "Graded open-cell aluminium foam core sandwich beams," *Materials Science and Engineering: A*, vol. 404, no. 1-2, p. 9, 2005.

[24] Y. Conde, A. Pollien, and A. Mortensen, "Functional grading of metal foam cores for yield-limited lightweight sandwich beams," *Scripta Materialia*, vol. 54, no. 4, p. 539, 2006.

[25] A. H. Brothers and D. C. Dunand, "Mechanical properties of a density-graded replicated aluminum foam," *Materials Science & Engineering A*, vol. 489, no. 1-2, pp. 439–443, 2008.

[26] J. L. Yu, J. R. Li, and S. S. Hu, "Strain-rate effect and microstructural optimization of cellular metals," *Mechanics of Materials*, vol. 38, no. 1-2, pp. 160–170, 2006.

[27] S. Li, X. Li, Z. Wang, G. Wu, G. Lu, and L. Zhao, "Finite element analysis of sandwich panels with stepwise graded aluminum honeycomb cores under blast loading," *Composites Part A: Applied Science and Manufacturing*, vol. 80, pp. 1–12, 2016.

[28] H. Zhou, Y. Wang, X. Wang, Z. Zhao, and G. Ma, "Energy absorption of graded foam subjected to blast: a theoretical approach," *Materials & Design*, vol. 84, pp. 351–358, 2015.

[29] R. Dou, S. Qiu, Y. Ju, and Y. Hu, "Simulation of compression behavior and strain-rate effect for aluminum foam sandwich panels," *Computational Materials Science*, vol. 112, pp. 205–209, 2016.

[30] G. W. Ma, Z. Q. Ye, and Z. S. Shao, "Modeling loading rate effect on crushing stress of metallic cellular materials," *International Journal of Impact Engineering*, vol. 36, no. 6, pp. 775–782, 2009.

[31] K. Li, X.-L. Gao, and G. Subhash, "Effects of cell shape and strut cross-sectional area variations on the elastic properties of three-dimensional open-cell foams," *Journal of the Mechanics and Physics of Solids*, vol. 54, no. 4, pp. 783–806, 2006.

[32] Z. Zheng, C. Wang, J. Yu, S. R. Reid, and J. J. Harrigan, "Dynamic stress-strain states for metal foams using a 3D cellular model," *Journal of the Mechanics and Physics of Solids*, vol. 72, pp. 93–114, 2014.

[33] D. Weaire and J. P. Kemrode, "On the distribution of cell areas in a Voronoi network," *Philosophical Magazine B*, vol. 53, pp. 101–105, 1986.

[34] X. Liu, X. Tian, T. Lu, D. Zhou, and B. Liang, "Blast resistance of sandwich-walled hollow cylinders with graded metallic foam cores," *Composite Structures*, vol. 94, pp. 2489–2493, 2012.

[35] D. S. Cheng, C. W. Hung, and S. J. Pi, "Numerical simulation of near-field explosion," *Tamkang Journal of Science and Technology*, vol. 16, no. 1, pp. 61–67, 2013.

[36] J. Kang, S. Shi, and C. Jin, "Theoretical analysis of attenuating shock wave pressure of aluminum foam," *Vibration and Shock*, vol. 29, no. 12, pp. 128–131, 2010.